IEEE Access
Multidisciplinary | Rapid Review | Open Access Journal

Received June 17, 2019, accepted August 16, 2019, date of publication August 27, 2019, date of current version September 9, 2019.

Digital Object Identifier 10.1109/ACCESS.2019.2937919

A Novel Enhanced Roll-Angle Measurement System Based on a Transmission Grating Autocollimator

WENRAN REN, JIWEN CUI, AND JIUBIN TAN

Center of Ultra-Precision Optoelectronic Instrument Engineering, Harbin Institute of Technology, Harbin 150080, China

Corresponding author: Jiwen Cui (cuijiwen@hit.edu.cn)

This work was supported in part by the Heilongjiang Province Outstanding Youth Science Fund Project under Grant HSF20190040.

ABSTRACT A resolution-enhanced roll-angle measurement system based on a transmission grating autocollimator is proposed. The measurement principle is analyzed in detail. The system uses a transmission grating and a mirror group to produce a pair of central symmetric differential measurement beams that enable the measurement of roll angle. Because the measurement beams transmit through the rotating grating twice, the resolution is enhanced compared to conventional grating autocollimation methods with the same device. The roll-angle resolution reached 0.1 arcsec. Additionally, the effect of laser beam drift on the stability of angular measurement is effectively suppressed by using differential measurement method, the stability of the proposed grating autocollimator after the differential measurement is 0.11 arcsec.

INDEX TERMS Autocollimator, roll angle measurement, laser drift, resolution.

I. INTRODUCTION

Precision angle measurement systems play an important role in precision manufacturing and equipment [1], precision motion control [2], [3], surface metrology [4], precision instrument calibration [5], and other precision measurement areas. The three geometric angular errors in precision measurements are the angular errors around three axes that correspond to pitch, yaw, and roll. Substantial research of angle measurement systems has been performed, including autocollimation [6]–[8], laser interference [9]–[12], total internal reflection [13]–[15], and fiber optic sensors [16], [17]. These methods can accurately determine both pitch and yaw by measuring beam-path- or beam-direction-changes. However, because roll-angle changes alter neither optical-path nor light-beam direction, most of these systems/sensors cannot measure roll angles.

Based on previous research of roll-angle measurements, optical methods can be divided into four categories. The first category, diffraction-grating-based autocollimation [18]–[20], use diffraction gratings as reflectors, and converts roll to a directional change of the ± 1st order diffraction beam. This direction change can be detected by autocollimation. The second method is based on polarization detection and uses a wave plate and a polarizer to enable the measurement [21]–[23]. The wave plate is the roll sensor: when the wave plate rolls, the intensity of the beam passing through the polarizer after the wave plate changes according to calculations made through Jones matrices. The roll error can be obtained by detecting the intensity of the beam. The third method is based on geometric relation transformation [24]. It uses a cube corner retro-reflector as angle sensor, which can convert roll into the movement of a light spot on a two-dimensional position sensitive detector or CCD. The roll error can be obtained by detecting the movement of the light spot during the measurement period. The fourth category is based on heterodyne interferometry [25], [26]. It uses a wedge prism and a wedge mirror as angle sensor. Changes of the optical path in the interferometric arms that are caused by roll are differential. They are converted into a phase shift, and the roll is obtained by detecting the phase shift.

Most of these methods are difficult to combine with two-dimensional angle measurements system to enable three-dimensional angle measurement – with one exception: the grating-based autocollimator proposed by Gao *et al.* [19]. While this method enables three-dimensional angle measurements, the roll resolution is lower than pitch and yaw when done with the same measurement system, theoretically.

The associate editor coordinating the review of this article and approving it for publication was Bora Onat.

In addition, the non-parallelism of three diffracted beams makes the system bulky, and the signal-detection part is difficult to install.

In this paper, we investigate a novel grating autocollimator for roll-angle measurements. The grating autocollimator utilizes a transmission grating as angle sensor, and position-sensitive detectors (PSD) for measurements. In this system, the two measurement beams pass through a transmission grating twice, which can double the measurement resolution and eliminates the non-parallelism of the two measurement beams. Furthermore, we use a differential measurement to eliminate the measurement error caused by light-source drifts, which can realize accurate and stable measurements.

II. MEASUREMENT PRINCIPLE

A. GRATING AUTOCOLLIMATOR

A typical grating autocollimator for roll-angle measurements is shown in Fig. 1. A collimated laser beam hits a transmission grating, which is mounted on a rotary stage. This generates a 1st-order diffracted beam and a −1st-order diffracted beam. The +1 and −1 order beams are focused by collimating lenses. The focused beams are detected by PSD_1 and PSD_2, respectively. Both PSD_1 and PSD_2 are located at the focal plane of the collimating lens so they can detect displacements of the diffracted beam focused on the detectors.

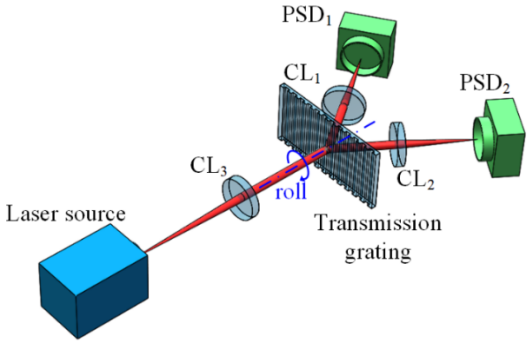

FIGURE 1. Schematic of the grating autocollimator for roll measurement.

Using the autocollimation- and diffraction-principle, the roll angle can be given as

$$\tan\gamma = \frac{g(\Delta y_1 - \Delta y_2)}{2f\lambda} \tag{1}$$

where f is the focal length of the collimating lens, λ is the wavelength of the laser source and g is the grating period of the transmission grating, Δy_1 is the vertical displacement of the spot detected by PSD_1, Δy_2 is the vertical displacement of the spot detected by PSD_2.

Because γ is a small angle, Eq. (1) can be simplified to

$$\gamma \approx \tan\gamma = \frac{g(\Delta y_1 - \Delta y_2)}{2f\lambda} \tag{2}$$

So the measurement resolution for roll, using Eq. (2), is given by

$$\Delta\gamma = \frac{\Delta y}{f\lambda/g} \tag{3}$$

where Δy is the displacement resolution of PSD_1 and PSD_2.

It can be seen form Eq. (2) that the accurate roll-angle γ can indeed be detected with the grating autocollimator. As shown in Eq. (3), due to the coefficients λ/g, the resolution for the roll measurement is below both pitch and yaw using autocollimation with the same device (i.e. same PSD and collimating lens). To decrease resolution differences between roll, pitch and yaw, we introduce a new measurement method. This method also improves the roll angle measurement resolution, and it makes the measurement system more compact.

B. THE PROPOSED GRATING AUTOCOLLIMATOR

A schematic of the proposed grating autocollimator is shown in Fig. 2. The laser beam from a laser source (LS) is collimated by a collimating lens (CL_1) after reflected by a reflect mirror (RM_1). The collimated laser beam then hits a transmission grating (TG), which is mounted on the rotary stage and generates both a 1st-order diffracted beam and -1st-order diffracted beam. Both beams are reflected by an assembly mirror group (AMG) which produces two beams that are parallel to the ±1st order diffracted beams, respectively. The AMG consists of two reflected mirrors (RM_2 and RM_3) and it is stationary. After reflected by the AMG, the beams hit the TG again, producing two measurement beams that are parallel to the collimated laser beam. The two measurement beams are focused by two collimating lenses (CL_2 and CL_3) and detected by PSD_1 and PSD_2. Compared to the grating autocollimator system shown in Fig. 1, the AMG is the only addition in our system. It ensures that the incident light and the outgoing light are parallel, while the propagation direction is opposite. This means that the outgoing beams can pass through the TG twice and ensure that the two measurement beams are parallel to the light-source beam.

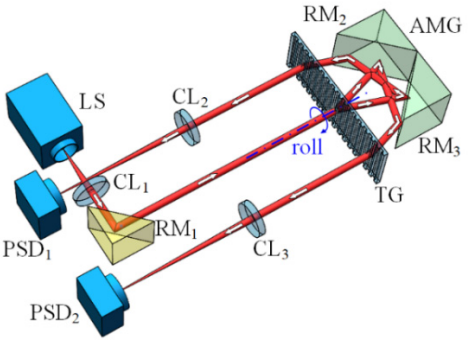

FIGURE 2. Schematic of the proposed grating autocollimator for roll measurements.

Fig. 3 shows a schematic of the displacements of the diffracted beam spots caused by the angular motion of the stage. A_0 and B_0 are the initial positions of the 1st-order and the -1st-order diffracted beam spots, respectively. A_1 and B_1 are the positions of the 1st-order and the -1st-order diffracted beam spots, respectively, when γ (the roll-angle displacement) occurs.

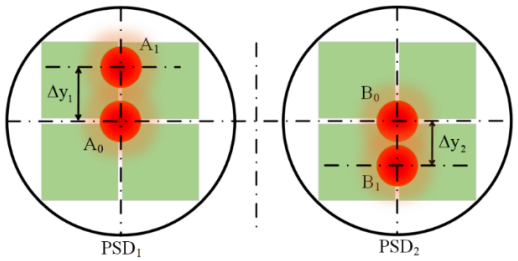

FIGURE 3. Displacements of the light spots on the detectors caused by the angular motions.

The measurement principle of the grating autocollimator is analyzed using the transformation matrix based on the reflection- and diffraction-principle. The grating coordinate-system is converted from the laboratory coordinate-system because of the occurrence of a roll angle γ. The transformation matrix from the laboratory coordinate-system to the grating coordinate-system for a roll angle γ is denoted by ${}^{G}R_{L}$. It can be expressed by

$$ {}^{G}R_{L} = \begin{bmatrix} \cos\gamma & \sin\gamma & 0 \\ -\sin\gamma & \cos\gamma & 0 \\ 0 & 0 & 1 \end{bmatrix} \tag{4} $$

The transformation matrix for the conversion from the grating coordinate-system to the laboratory coordinate-system for the roll angle γ is denoted by ${}^{L}R_{G}$. It can be expressed by

$$ {}^{L}R_{G} = \begin{bmatrix} \cos\gamma & -\sin\gamma & 0 \\ \sin\gamma & \cos\gamma & 0 \\ 0 & 0 & 1 \end{bmatrix} \tag{5} $$

The transformation matrix of RM_2 and RM_3 can be expressed as

$$ R_2 = \begin{bmatrix} -1 & 0 & 0 \\ 0 & 0 & 1 \\ 0 & -1 & 0 \end{bmatrix}, \quad R_3 = \begin{bmatrix} 1 & 0 & 0 \\ 0 & 0 & 1 \\ 0 & 1 & 0 \end{bmatrix} \tag{6} $$

The direction cosine A_1 (in laboratory coordinates) of the collimated laser-beam, coming from the laser source with an angle drift δ in vertical direction, can be expressed as

$$ A_1 = \begin{bmatrix} 0 \\ \sin\delta \\ \cos\delta \end{bmatrix} \tag{7} $$

The direction cosine A_1' (in grating coordinates) of the collimated laser-beam, with an angle drift δ in vertical direction, can be expressed by

$$ A_1' = {}^{G}R_{L}A_1 = \begin{bmatrix} \sin\gamma\sin\delta \\ \cos\gamma\sin\delta \\ \cos\delta \end{bmatrix} \tag{8} $$

Based on the diffraction principle, the direction cosine A_2' (in grating coordinates) of the 1st-order diffracted beam can be expressed by

$$ A_2' = \begin{bmatrix} \sin\phi \\ \cos\gamma\sin\delta \\ \sqrt{1-\sin^2\phi-(\cos\gamma\sin\delta)^2} \end{bmatrix} \tag{9} $$

where ϕ is the diffraction angle of the 1st-order diffracted beam, and $\sin\phi$ can be expressed by

$$ \sin\phi = \frac{\lambda}{g} \tag{10} $$

where λ is the wavelength of the laser source and g is the grating period of the transmission grating.

The direction cosine A_2 (in laboratory coordinates) of the 1st-order diffracted beam can be expressed by

$$ A_2 = {}^{L}R_{G}A_2' = \begin{bmatrix} \cos\gamma\sin\phi-\sin\gamma\cos\gamma\sin\delta \\ \sin\gamma\sin\phi+\cos^2\gamma\sin\delta \\ \sqrt{1-\sin^2\phi-(\cos\gamma\sin\delta)^2} \end{bmatrix} \tag{11} $$

The 1st-order diffracted beam then proceeds to the AMG and is reflected by RM_2 and RM_3, the direction cosine A_3 (in laboratory coordinates) of the 1st-order diffracted beam, after reflection by the AMG, can be expressed as

$$ A_3 = R_3R_2A_2 = \begin{bmatrix} \sin\gamma\cos\gamma\sin\delta-\cos\gamma\sin\phi \\ \sin\gamma\sin\phi+\cos^2\gamma\sin\delta \\ -\sqrt{1-\sin^2\phi-(\cos\gamma\sin\delta)^2} \end{bmatrix} \tag{12} $$

After reflection by the AMG, the beam hits the TG the second time. The direction cosine A_3' (in grating coordinate) of the incident beam can be given as

$$ A_3' = {}^{G}R_{L}A_3 = \begin{bmatrix} \sin\gamma\sin\delta-\sin\phi\cos2\gamma \\ \sin\phi\sin2\gamma+\cos\gamma\sin\delta \\ -\sqrt{1-B^2-C^2} \end{bmatrix} \tag{13} $$

where

$B = \sin\gamma\sin\delta - \sin\phi\cos2\gamma$

$C = \sin\phi\sin\ 2\gamma + \cos\gamma\sin\delta$

After grating diffraction, the 1st-order diffracted beam of the second diffraction is selected to be the first measurement beam because it is parallel to the collimated laser-beam from the laser source. Using the diffraction principle, the direction cosine A_4' (in grating coordinates), of the first measurement beam, can be given as

$$ A_4' = \begin{bmatrix} 2\sin^2\gamma\sin\phi+\sin\gamma\sin\delta \\ \sin\phi\sin2\gamma+\cos\gamma\sin\delta \\ -\sqrt{1-D^2-E^2} \end{bmatrix} \tag{14} $$

where

$D = 2\sin^2\gamma\sin\phi + \sin\gamma\sin\delta$

$E = \sin\phi\sin\ 2\gamma + \cos\gamma\sin\delta$

Subsequently, the direction cosine of the first measurement beam must be transformed into laboratory coordinates because the detection system was designed and installed using the laboratory coordinate system. This must be done such that the amount of change in the direction of the first measurement beam can be detected directly by the detector.

The direction cosine A_4 (in laboratory coordinates), can be expressed by

$$A_4 = {}^{L}R_G A_4{}' = \begin{bmatrix} 0 \\ 2\sin\gamma\sin\phi + \sin\delta \\ -\sqrt{1-(2\sin\gamma\sin\phi+\sin\delta)^2} \end{bmatrix} \quad (15)$$

The first measurement beam is detected by the PSD_1 after focusing by the CL_2. The displacement Δy_1 of the light spot on the PSD_1 can be derived using Eq. (15):

$$\Delta y_1 = f\frac{2\sin\gamma\sin\phi+\sin\delta}{\sqrt{1-(2\sin\gamma\sin\phi+\sin\delta)^2}} \quad (16)$$

Because both roll-angle γ and angular-drift δ are small, $\sqrt{1-(2\sin\gamma\sin\phi+\sin\delta)^2}$ is almost equal to 1, which means Eq. (16) can be simplified to

$$\sin\gamma = \frac{(\Delta y_1/f - \sin\delta)}{2\sin\phi} \quad (17)$$

Similarly, using the transformation matrix based on the reflection- and diffraction- principles, the second measurement beam, detected by PSD_2, is focused by CL_3. The displacement Δy_2 of the light spot on PSD_2 is given by

$$-\sin\gamma = \frac{(\Delta y_2/f - \sin\delta)}{2\sin\phi} \quad (18)$$

Using Eq. (17) and Eq. (18), the accurate roll-angle γ, which eliminates the interference of the angular drift δ, can be given by

$$\gamma \approx \sin\gamma = \frac{\Delta y_1 - \Delta y_2}{4f\sin\phi} \quad (19)$$

Substituting Eq. (10) into Eq. (19), we can obtain the roll angle γ, expressed by

$$\gamma = \frac{g(\Delta y_1 - \Delta y_2)}{4f\lambda} \quad (20)$$

As a result, the roll-measurement resolution, using Eq. (20), is given by

$$\Delta\gamma = \frac{g}{2f\lambda}\Delta y \quad (21)$$

Comparing (3) and (21), the resolution of the proposed grating autocollimator is twice the one of the grating autocollimator. In addition, as shown in Eq. (17) and Eq. (18), the roll angle γ and the angular drift δ (random error) can be separated from the roll angle. This means that the random error δ can be eliminated by the differential measurement see Eq. (19). Hence, both high accuracy and high stability were obtained. Because the two measurement beams are parallel to the collimated laser beam from the laser source, the measuring system is more compact and can be installed easily.

III. ERROR ANALYSIS OF MEASUREMENT SYSTEM

A. CROSSTALK ERROR CAUSED BY PITCH AND YAW

For the roll angle measurement system, the effect of pitch and yaw angles on the angle of roll cannot be ignored.

As shown in Fig. 4(a), when the TG rotates α around X-axis, the +1st diffraction angle θ_{+1} can be given by

$$\sin\theta_{+1} = \sin\phi + \sin\alpha \quad (22)$$

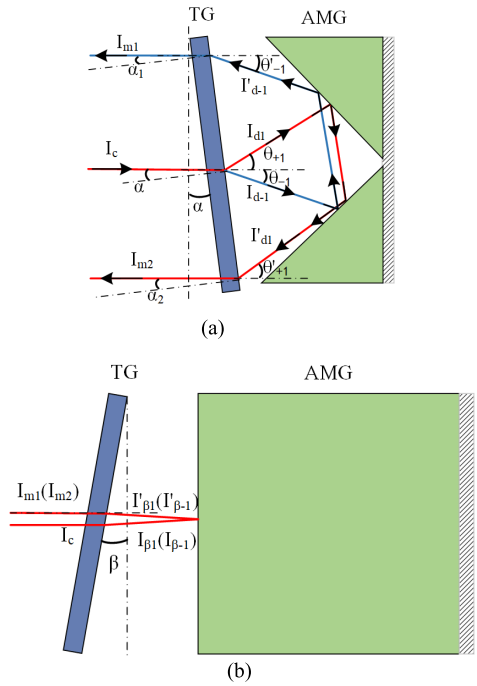

FIGURE 4. Schematic of beam path when pitch and yaw exist. (a) TG with pitch α; (b) TG with yaw β.

After being reflected by AMG, the incident angle of the reflected beam I'_{d1} is θ'_{+1}, and it equals to angle θ_{+1}. Then after being diffracted by TG, the diffraction angle of the second-time diffraction beam α_2 can be given by

$$\sin\alpha_2 = \sin\theta'_{+1} - \sin\phi = \sin\theta_{+1} - \sin\phi = \sin\alpha \quad (23)$$

So, the measurement beam I_{m2} is always parallel to beam I_c, even pitch angle exists. So it is with measurement beam I_{m1}. Hence, there is no crosstalk error caused by pitch angle for roll angle measurement.

As shown in Fig. 4(b), when the TG rotates β around Y-axis, the direction cosine B'_1 (in grating coordinates) of incident beam I_c with β can be given by

$$B'_1 = {}^{G}R_{L\beta}A = \begin{bmatrix} 1 & 0 & 0 \\ 0 & \cos\beta & \sin\beta \\ 0 & -\sin\beta & \cos\beta \end{bmatrix}\begin{bmatrix} 0 \\ 0 \\ 1 \end{bmatrix} = \begin{bmatrix} 0 \\ \sin\beta \\ \cos\beta \end{bmatrix} \quad (24)$$

where ${}^{G}R_{L\beta}$ is transformation matrix for the conversion from the laboratory coordinate-system to the grating

coordinate-system for the roll angle β. A is the direction cosine of beam I_c.

After being diffracted by TG, the direction cosine B'_2 (in grating coordinates) of +1st order diffraction beam $I_{\beta 1}$ is given by

$$B'_2 = \begin{bmatrix} \sin\phi \\ \sin\beta \\ \sqrt{1-\sin^2\phi-\sin^2\beta} \end{bmatrix} \tag{25}$$

Before being reflected by AMG, the direction cosine B_2 (in laboratory coordinates) of +1st order diffraction beam $I_{\beta 1}$ is given by

$$B_2 = {}^{L}R_{G\beta}B'_2 = \begin{bmatrix} 1 & 0 & 0 \\ 0 & \cos\beta & -\sin\beta \\ 0 & \sin\beta & \cos\beta \end{bmatrix}$$

$$B'_2 = \begin{bmatrix} \sin\phi \\ (\cos\beta - \sqrt{1-\sin^2\phi-\sin^2\beta})\sin\beta \\ \cos\beta\sqrt{1-\sin^2\phi-\sin^2\beta}+\sin^2\beta \end{bmatrix} \tag{26}$$

where ${}^{L}R_{G\beta}$ is transformation matrix for the conversion from the grating coordinate-system to the laboratory coordinate-system with yaw angle β.

After being reflected by AMG, the direction cosine B_3 (in laboratory coordinates) of reflected beam $I'_{\beta 1}$ is given by

$$B_3 = \begin{bmatrix} \sin\phi \\ -(\cos\beta - \sqrt{1-\sin^2\phi-\sin^2\beta})\sin\beta \\ -\cos\beta\sqrt{1-\sin^2\phi-\sin^2\beta}+\sin^2\beta \end{bmatrix} \tag{27}$$

The direction cosine B'_3 (in grating coordinates) of beam $I'_{\beta 1}$ is given by

$$B'_3 = {}^{G}R_{L\beta}B_3 = \begin{bmatrix} \sin\phi \\ -\sin\beta \\ -\sqrt{1-\sin^2\phi-\sin^2\beta} \end{bmatrix} \tag{28}$$

After the second-time diffraction, the direction cosine B'_4 (in grating coordinates) of I_{m2} is given by

$$B'_4 = \begin{bmatrix} 0 \\ -\sin\beta \\ -\cos\beta \end{bmatrix} \tag{29}$$

The direction cosine B_4 (in laboratory coordinates) of I_{m2} is given by

$$B'_4 = {}^{L}R_{G\beta}B'_4 = \begin{bmatrix} 0 \\ 0 \\ -1 \end{bmatrix} \tag{30}$$

Hence, So, the measurement beam I_{m2} is always parallel to beam I_c, even yaw angle exists. So it is with measurement beam I_{m1}. Hence, there is no crosstalk error caused by yaw angle for roll angle measurement.

B. EFFECTS OF ASSEMBLY ERRORS OF AMG

The AMG consists of two reflected mirrors. The mirror is very sensitive to the angle variation, so the assembly errors of the AMG are inevitable. If the AMG has no errors, the direction of the diffraction beam should remain unchanged after the beam passes through them, as shown in Fig. 5(a).

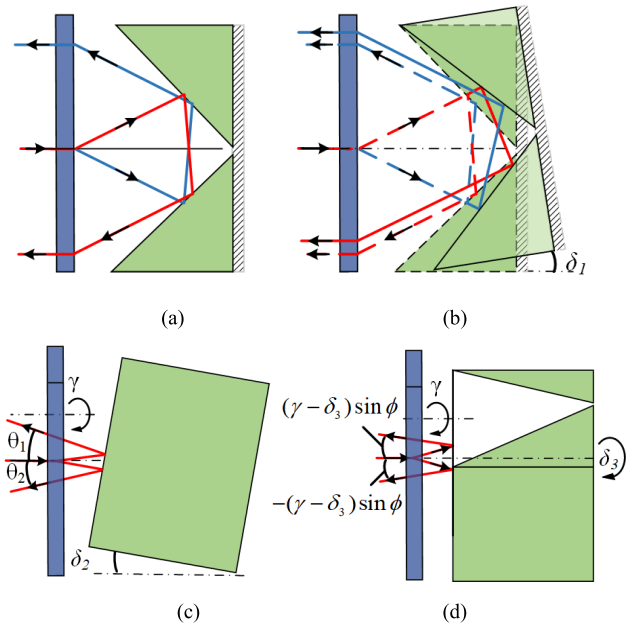

FIGURE 5. Assembly errors of AMG. (a) without assembly errors; (b) with pitch error δ_1; (c) with yaw error δ_2; (d) with roll error δ_3.

There would be three small assembly errors δ_1, δ_2 and δ_3 around X-, Y- and Z-axis, as shown in Figs. 5(b), 5(c) and 5(d). If there is an assembly error δ_1 around X-axis, the outgoing beam is still parallel to the incident beam, so the assembly error δ_1 has no effect on roll angle measurement.

If there is an assembly error δ_2 around Y-axis, using the transformation matrix based on the reflection- and diffraction-principle, the angle of measurement beam I_{m1} and I_{m2} in the vertical direction with roll angle γ can be expressed by

$$\sin\theta_1 = \sin(2\delta_2)(\sin(45-\phi)+\sin(45+\phi)) + \sin(2\gamma)\sin\phi \tag{31}$$

$$\sin\theta_2 = \sin(2\delta_2)(\sin(45-\phi)+\sin(45+\phi)) - \sin(2\gamma)\sin\phi \tag{32}$$

Using Eqs. (31) and (32), the assembly error δ_2 can be eliminated by difference operation

$$\sin(2\gamma) = \frac{\sin\theta_1 - \sin\theta_2}{2\sin\phi} \tag{33}$$

So, the assembly error δ_2 has no effect on roll angle measurement.

If there is an assembly error δ_3 around Z-axis, as shown in Fig. 5(d). when the TG rotates γ around Z-axis, the relative roll angle between the grating and AMG is γ-δ_3.

Hence, similar to section 2.2, the relative roll angle can be given

$$\gamma - \delta_3 = \frac{g(\Delta y_1 - \Delta y_2)}{4f\lambda} \tag{34}$$

However, error δ_3 is a constant since the AMG is an assembly, so the error brings only a constant deflection of measurement beam. The direction of measurement beams varies only with the angular change of TG. So, the AMG is quite compatible with the assembly errors, which means that the assembly errors of the AMG have no effect on roll angle measurement.

IV. EXPERIMENT AND RESULTS

To verify the performance of the proposed grating autocollimator, an experimental setup based on the schematic diagram in Fig. 2 was assembled and shown in Fig. 6. In our experiments, a He-Ne gas laser with a wavelength of 635 nm was chosen as the light source. A transmission grating, which serves as a roll-sensing element, was mounted on an angle-generating device. The constant g of the chosen transmission grating was 4 μm. The focal length of the collimating lens is 1800 mm.

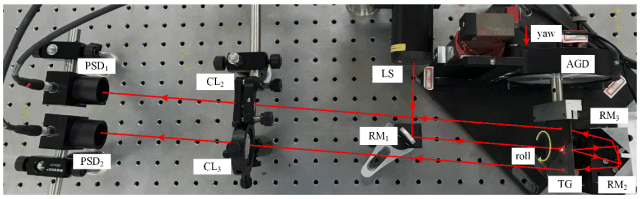

FIGURE 6. Experimental setup for roll angle measurement.

A. CONSISTENCY TEST OF LASER SOURCE DRIFTS OF TWO MEASUREMENT BEAMS

As shown in Eqs. (17) and (18), to obtain the accurate roll-angle γ by using the the differential measurement method, the measurement errors of the two PSDs caused by angular-drift δ should be consistent, this is the premise that the differential measurement method can be applied. In order to verify that the differential measurement method can effectively eliminate the effect of laser source drift on the measurement results, a consistency tests of laser source drifts of two measurement beams are carried out. As shown in Fig. 2, before the laser source is incident on the TG, it is reflected by a reflect mirror (RM_1). We fix the RM_1 on rotary stage to simulate regular beam drift and compare the response of two measurement beams to the drift. The rotation steps of the rotary stage and the corresponding directional changes of two measurement beams are shown in Fig. 7. It can be seen that the directions of the two measurement beams have consistent directional changes with the direction of the incident beam.

B. RESOLUTION IMPROVEMENT EFFECTIVENESS TEST

As describe in Part 2, using the Eqs. (3) and (21), the measurement resolution of our system is doubled compares to the typical grating autocollimator, theoretically. That is, for the same angle change, the output of PSDs in proposed system is doubled compares to the typical grating autocollimator. In the experiment, the rotation step of the rotary stage is 10 arcsec from 0 to 50 arcsec, the outputs of the two systems are shown in Fig. 8. It can be seen that the output of the proposed system is doubled compares to the typical grating autocollimator.

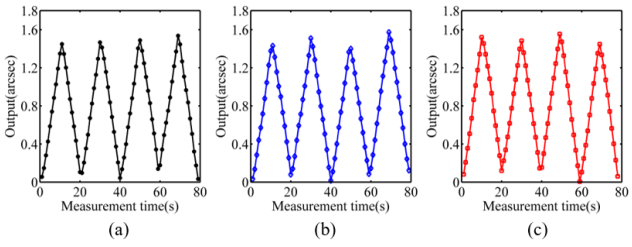

FIGURE 7. Directional changes of measurement beams with incident beam. (a) Incident beam; (b) PSD_1; (3) PSD_2.

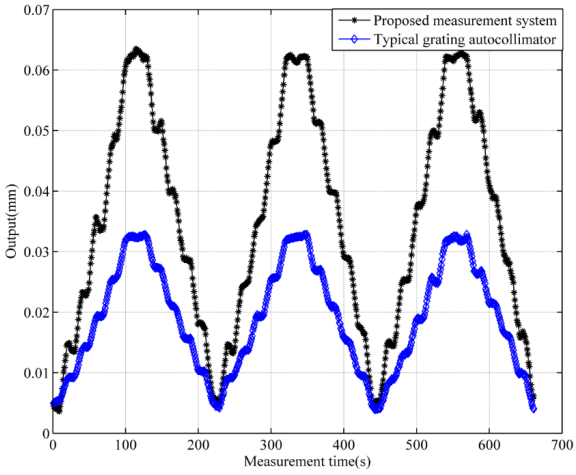

FIGURE 8. Outputs of the two measurement systems.

C. RESOLUTION TEST OF THE PROPOSED GRATING AUTOCOLLIMATOR

An angular deflection device with a flexible hinge was used to measure the resolution of the proposed grating autocollimator. The resolution of the PSD in our system is test before the experiment, the results of the test is shown in Fig. 9(a). It can be seen that the resolution of the PSD is less than 300 nm. The focal length of the collimating lens is 1800mm in our system. So, using the Eq. (21), the theoretical resolution of roll angle measurement is better than 0.109 arcsec. So, the step size of the rotary stage is 0.1 arcsec. The corresponding time interval for each step was 10 s. The output of the proposed grating autocollimator is shown in Fig. 9(b). The results show that the output of the roll angle γ can reveal each step clearly, which indicates that the resolution of the system is less than 0.1 arcsec.

D. STABILITY TEST OF THE PROPOSED GRATING AUTOCOLLIMATOR

The setup for the stability test is shown in Fig. 10. The experimental setup was placed on an air bearing stage in a

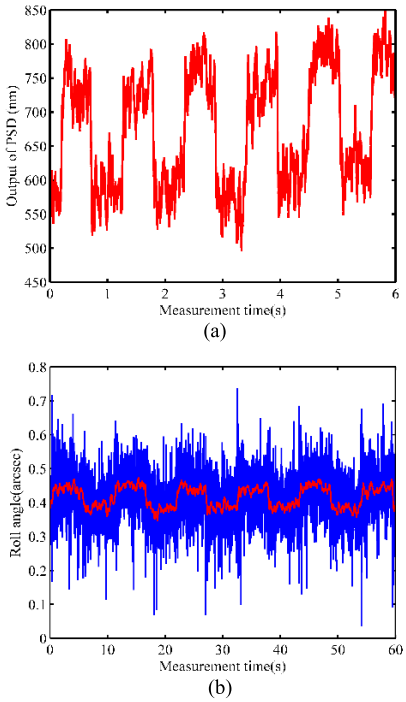

FIGURE 9. Results of the resolution test. (a) PSD; (b) proposed grating autocollimator.

clean room with constant temperature and vibration isolation. The results of the roll-angle measurement with and without angular drift, following the differential measurements, are shown in Fig. 10. The drift of the first and second measurement beams are 0.21 arcsec and 0.27 arcsec. The correlation coefficients, which reflect the consistency of the first and second measurement beams was 77.0%, and the stability of the proposed grating autocollimator after the differential measurement was 0.11 arcsec. In other words, the proposed grating autocollimator has very good measurement stability. As a result, it can be concluded that the proposed grating autocollimator can improve both measurement accuracy and measurement stability using the differential measurement.

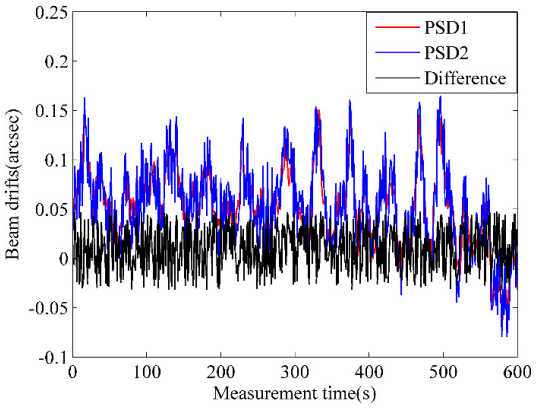

FIGURE 10. Stability test of the proposed grating autocollimator: Beam drifts of the first and the second measurement beams, and the difference between them.

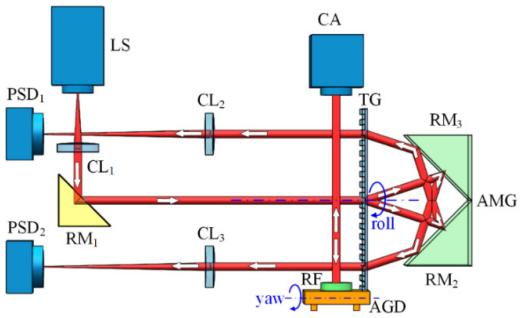

FIGURE 11. Schematic of the calibration experimental setup.

E. CALIBRATION OF THE PROPOSED GRATING AUTOCOLLIMATOR

A schematic diagram of the comparative experimental setup is shown in Fig. 11. The transmission grating and a reflector (RF) are orthogonally mounted on the angle-generating device (AGD). The reflector is a yaw-sensing element of a commercial autocollimator (CA) (ELCOMAT HR, MOLLER Co, GER). Because the transmission grating and the reflector was aligned orthogonally, the roll angle γ, which is detected by the proposed grating autocollimator, and the yaw angle β which is detected by the commercial autocollimator are consistent, and they can be read out simultaneously. The roll-angle range of the angle-generating device is 280 arcsec, and the step size is 28 arcsec. At the same time, 11 date groups were collected using the proposed grating autocollimator and the commercial autocollimator. The measurements are shown in Fig. 12.

As shown in Fig. 12, the output γ of the proposed grating autocollimator is identical with the output β. The residuals between them are shown in Fig. 12. The residual errors range from -0.48 to 0.70 arcsec, and the standard deviation is 0.41 arcsec for a range of 280 arcsec. Three factors produce most of the deviation: the measurement error of the CA, the error introduced by our roll-measurement system, and the random error caused by the environment. The measurement

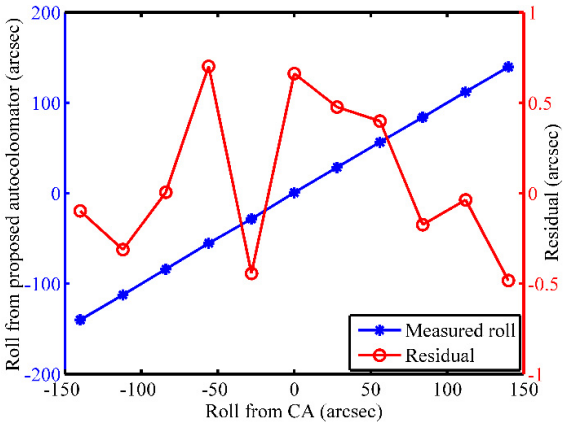

FIGURE 12. Roll obtained using the proposed grating autocollimator against roll obtained using the commercial autocollimator and the residual between them.

results show the feasibility of the new measurement method with the proposed system.

V. CONCLUSION

This paper proposed and verified a resolution enhanced grating autocollimator, which uses a novel configuration that includes a transmission grating and a mirror group for improved roll-angle measurements. The measurement resolution has been doubled because the measurement beams pass through the transmission grating twice. To verify the effect of the autocollimator, a test setup was built. A comparison with a commercial autocollimator indicates the feasibility of the proposed grating autocollimator. A resolution test experiment was performed and an enhanced resolution of 0.1 arcsec was obtained. Furthermore, very stable measurements can be obtained thanks to the differential measurement method. Stability tests of the proposed grating autocollimator were performed, which indicate a stability of 0.11 arcsec. However, due to the limitation of diffraction angle and AMG size, the moving distance of the grating will not be very long. So, the measurement system is not suitable for measuring the angular change of the long-distance linear stage.

REFERENCES

[1] H. Schwenke, W. Knapp, H. Haitjema, A. Weckenmann, R. Schmitt, and F. Delbressine, "Geometric error measurement and compensation of machines—An update," *CIRP Ann.*, vol. 57, no. 2, pp. 660–675, Sep. 2008.
[2] W. Gao, S. W. Kim, H. Bosse, H. Haitjema, Y. L. Chen, X. D. Lu, W. Knapp, A. Weckenmann, W. T. Estler, and H. Kunzmann, "Measurement technologies for precision positioning," *CIRP Ann.*, vol. 64, no. 2, pp. 773–796, Mar. 2015.
[3] J. W. Kim, C.-S. Kang, J.-A. Kim, T. Eom, M. Cho, and H. J. Kong, "A compact system for simultaneous measurement of linear and angular displacements of nano-stages," *Opt. Express*, vol. 15, no. 24, pp. 15759–15766, Nov. 2007.
[4] G. Ehret, M. Schulz, M. Stavridis, and C. Elster, "Deflectometric systems for absolute flatness measurements at PTB," *Meas. Sci. Technol.*, vol. 23, no. 9, Jul. 2012, Art. no. 094007.
[5] B. J. Eves, "The NRC autocollimator calibration facility," *Metrologia*, vol. 50, no. 5, p. 433, Aug. 2013.
[6] F. Zhu, J. Tan, and J. Cui, "Common-path design criteria for laser datum based measurement of small angle deviations and laser autocollimation method in compliance with the criteria with high accuracy and stability," *Opt. Express*, vol. 21, no. 9, pp. 11391–11403, May 2013.
[7] Y.-L. Chen, Y. Shimizu, J. Tamada, Y. Kudo, S. Madokoro, K. Nakamura, and W. Gao, "Optical frequency domain angle measurement in a femtosecond laser autocollimator," *Opt. Express*, vol. 25, no. 14, pp. 16725–16738, Jul. 2017.
[8] J. Yuan and X. Long, "CCD-area-based autocollimator for precision small-angle measurement," *Rev. Sci. Instrum.*, vol. 74, no. 3, pp. 1362–1365, Mar. 2003.
[9] D. Zheng, X. Wang, and Z. Li, "Accuracy analysis of parallel plate interferometer for angular displacement measurement," *Opt. Laser Technol.*, vol. 40, no. 1, pp. 6–12, May 2007.
[10] E. Zhang, B. Chen, J. Sun, L. Yan, and S. Zhang, "Laser heterodyne interferometric system with following interference units for large X-Y-θ planar motion measurement," *Opt. Express*, vol. 25, no. 12, pp. 13684–13690, Jun. 2017.
[11] M. Pisani, "Multiple reflection Michelson interferometer with picometer resolution," *Opt. Express*, vol. 16, no. 26, pp. 21558–21563, Dec. 2008.
[12] S.-T. Lin, S.-L. Yeh, and C.-W. Chang, "Low-coherent light-source angular interferometer using a square prism and the angular-scanning technique," *Opt. Lett.*, vol. 33, no. 20, pp. 2344–2346, Oct. 2008.
[13] Y. Liu, C. Kuang, and Y. Ku, "Small angle measurement method based on the total internal multi-reflection," *Optics Laser Technol.*, vol. 44, no. 5, pp. 1346–1350, Jul. 2012.
[14] J.-Y. Lin and Y.-C. Liao, "Small-angle measurement with highly sensitive total-internal-reflection heterodyne interferometer," *Appl. Opt.*, vol. 53, no. 9, pp. 1903–1908, Mar. 2014.
[15] C.-J. Chen and P. D. Lin, "High-accuracy small-angle measurement of the positioning error of a rotary table by using multiple-reflection optoelectronic methodology," *Proc. SPIE*, vol. 46, no. 11, Nov. 2007, Art. no. 113604.
[16] A. Khiat, F. Lamarque, C. Prelle, N. Bencheikh, and E. Dupont, "High-resolution fibre-optic sensor for angular displacement measurements," *Meas. Sci. Technol.*, vol. 21, no. 2, Jan. 2010, Art. no. 025306.
[17] J. M. S. Sakamoto, C. Kitano, G. M. Pacheco, and B. R. Tittmann, "High sensitivity fiber optic angular displacement sensor and its application for detection of ultrasound," *Appl. Opt.*, vol. 51, no. 20, pp. 4841–4851, Jul. 2012.
[18] X. Li, W. Gao, H. Muto, Y. Shimizu, S. Ito, and S. Dian, "A six-degree-of-freedom surface encoder for precision positioning of a planar motion stage," *Precis. Eng.*, vol. 37, no. 3, pp. 771–781, Jul. 2013.
[19] W. Gao, Y. Saito, H. Muto, Y. Arai, and Y. Shimizu, "A three-axis autocollimator for detection of angular error motions of a precision stage," *CIRP Ann.*, vol. 60, no. 1, pp. 515–518, 2011.
[20] Y. Saito, Y. Arai, and W. Gao, "Detection of three-axis angles by an optical sensor," *Sens. Actuators A, Phys.*, vol. 150, no. 2, pp. 175–183, Mar. 2009.
[21] S. R. Gillmer, X. Yu, C. Wang, and J. D. Ellis, "Robust high-dynamic-range optical roll sensing," *Opt. Lett.*, vol. 40, no. 11, pp. 2497–2500, May 2015.
[22] S. R. Gillmer, J. Martínez-Rincón, and J. D. Ellis, "Anomalous vibration suppression in a weak-value-emulated heterodyne roll interferometer," *Opt. Express*, vol. 26, no. 22, pp. 29311–29318, Oct. 2018.
[23] P. Zhang, Y. Wang, C. Kuang, S. Li, and X. Liu, "Measuring roll angle displacement based on ellipticity with high resolution and large range," *Opt. Laser Technol.*, vol. 65, pp. 126–130, Jan. 2015.
[24] Y. Zhai, Q. Feng, and B. Zhang, "A simple roll measurement method based on a rectangular-prism," *Opt. Laser Technol.*, vol. 44, no. 4, pp. 839–843, Jun. 2012.
[25] Y. Le, W. Hou, K. Hu, and K. Shi, "High-sensitivity roll-angle interferometer," *Opt. Lett.*, vol. 38, no. 18, pp. 3600–3603, Sep. 2013.
[26] K. Shi, J. Su, and W. Hou, "Roll angle measurement system based on differential plane mirror interferometer," *Opt. Express*, vol. 26, no. 16, pp. 19826–19834, Jul. 2018.

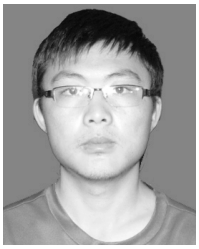

WENRAN REN received the B.S. and M.S. degrees in instrumentation science and technology from the Harbin Institute of Technology (HIT), Harbin, China, in 2014 and 2015, respectively. He is currently pursuing the Ph.D. degree. His research interests include angle measurement and optical sensor.

JIWEN CUI received the B.S., M.S., and Ph.D. degrees from the Harbin Institute of Technology (HIT), in 1998, 2000, and 2005, respectively, where he is currently a Professor and the Director of the Experimental Center of Optoelectronic Information. His current research interests include ultra-precision optical sensor and instrument technology.

JIUBIN TAN received the Ph.D. degree from the Harbin Institute of Technology (HIT), Harbin, China, in 1991, where he is currently a Professor and an Academician of the Chinese Academy of Engineering. His current research interests include ultra-precision instrument engineering and ultra-precision machining measurement equipment and technology. He was a recipient of the National Invention Award of China as a first inventor, in 2006.